Rock Mechanics 1, 5–30 (1969)

Deformation of Rock Salt in Openings Mined for the Disposal of Radioactive Wastes*

By

T. F. Lomenick and **R. L. Bradshaw**

With 15 Figures

(Received January 8, 1969)

Summary — Zusammenfassung — Résumé

Deformation of Rock Salt in Openings Mined for the Disposal of Radioactive Wastes. With the storage of high-level radioactive waste in salt structures, unique mine stability problems will occur as a result of the elevated temperatures. To predict flow in rock salt, scale models of salt pillars and their surrounding rooms were fabricated from cores taken in the Carey salt mine, Lyons, Kansas. Tests were conducted at temperatures of 22.5°, 60°, 100°, and 200°C for axial loads of 2000, 4000, 6000, 8000, and 10 000 psi at each temperature. These tests showed that marked increases occur in the rates of deformation of salt pillars at high loads and especially at elevated temperatures. For all combinations of axial loads and temperatures, it was observed that there is initially a high rate of deformation that diminishes with time. Creep rates were found to continue to decrease even after more than 3 years of testing. An empirical relationship between pillar deformation, stress, temperature, and time was developed from the tests and is expressed as

$$\dot{\varepsilon} = 0.39 \cdot 10^{-37}\, T^{9.5}\, \sigma^{3.0}\, t^{-0.70},$$

$$\varepsilon = 1.30 \cdot 10^{-37}\, T^{9.5}\, \sigma^{3.0}\, t^{0.30},$$

where $\dot{\varepsilon}$ = strain rate (in./in./hr), ε = cumulative deformation (in./in.), T = absolute temperature (°K), σ = average pillar stress (psi), and t = time (hr).

For comparative purposes, model pillar tests were conducted on samples of bedded salt, as well as dome salt from six different mines in the United States and from the anticlinal structure of the Asse II salt mine in Northeast Germany. In general, the deformational behavior for the various types of salt was similar at room temperature as well as at elevated temperature even though some variations in the rates of deformation were observed.

From model tests it was also observed that greatly accelerated rates of deformation will occur in excavated cavities where thin shale beds occur in the pillars at the roof and floor interfaces. Since the shales serve as friction reducers, effective confining stresses in the roof and floor are not transmitted into the pillars; thus the pillars under these conditions are weaker than where shale partings are not present at the tops and bottoms of the pillars.

Verformung von Steinsalz in Schächten zur Beseitigung radioaktiver Abfälle. Bei der Lagerung stark radioaktiver Abfälle in Salzbergwerken treten wegen der erhöhten Temperaturen neuartige Stabilitätsprobleme auf. Um das Fließen im Steinsalz vorauszusagen, wurden maßstabgetreue Modelle von Salzträgern und ihrer umgebenden Räume aus Bohrkernen

* Research sponsored by the U. S. Atomic Energy Commission under contract with the Union Carbide Corporation.

des Carey-Salzbergwerkes in Lyons, Kansas, hergestellt. Die Versuche wurden bei Temperaturen von 22,5°, 60°, 100° und 200°C und bei Achsenbelastungen von 2000, 4000, 6000, 8000 und 10000 Pfund per Quadratinch (psi) durchgeführt. Sie zeigten, daß bei hohen Belastungen und besonders bei erhöhten Temperaturen die Verformung der Salzträger merklich zunimmt. Bei allen Achsenbelastungs- und Temperaturkombinationen wurde beobachtet, daß die Verformungsgeschwindigkeit nach einem hohen Anfangswert mit der Zeit abnimmt. Die Kriechgeschwindigkeiten nahmen noch nach mehr als drei Jahren ab. Eine empirische Abhängigkeit zwischen Trägerverformung, Spannung, Temperatur und Zeit wurde aus den Tests gewonnen:

$$\dot{\varepsilon} = 0.39 \cdot 10^{-37}\, T^{9.5}\, \sigma^{3.0}\, t^{-0.70},$$

$$\varepsilon = 1.30 \cdot 10^{-37}\, T^{9.5}\, \sigma^{3.0}\, t^{0.30},$$

mit $\dot{\varepsilon}$ = Verformungsgeschwindigkeit (in./in./hr), ε = kumulative Verformung (in./in.), T = absolute Temperatur (°K), σ = mittlere Trägerspannung (psi) und t = Zeit (hr).

Vergleichshalber wurden Modellversuche an Proben von Salzlagern sowie an Kuppelsalz aus sechs verschiedenen Bergwerken in den Vereinigten Staaten und aus dem antiklinalen Salz des Bergwerkes Asse II im nordöstlichen Teil Deutschlands durchgeführt. Im allgemeinen war das Verformungsverhalten der verschiedenen Salzarten bei Zimmertemperatur wie bei erhöhter Temperatur ähnlich, obwohl einige Abweichungen der Verformungsgeschwindigkeiten beobachtet wurden.

In weiteren Versuchen wurde beobachtet, daß die Verformungen in Hohlräumen, wo dünne Schieferschichten an den Dach- und Bodenzwischenflächen der Träger auftraten, wesentlich beschleunigt waren. Da die Schieferstücke als Reibungsreduktionsmittel fungieren, werden wirksame beschränkende Spannungen auf die Träger nicht übertragen; daher sind die Träger unter diesen Umständen schwächer als in Fällen in denen keine Schiefertrennungen an den oberen und unteren Enden der Träger vorhanden sind.

Déformation du sel gemme dans des cavités minières pour des déchets radioactifs. Lors du stockage des déchets de haute radioactivité dans les formations géologiques de sel gemme les températures élevées causent des problèmes spéciaux de stabilité. Pour prévoir l'écoulement dans les formations de sel gemme on a construit des modèles réduits de piliers de sel à partir de carottes obtenues dans la mine de sel Carey à Lyons, Kansas. On a fait des essais à des températures de 22,5° 60°, 100° et 200°C, pour des charges axiales de 2000, 4000, 6000, 8000, 10000 psi à chaque température. Ces essais ont montré que les hautes charges augmentent sensiblement les vitesses de déformation, en particulier aux températures élevées. Pour toutes les combinaisons de charges axiales et de températures, on a observé qu'il y a au début une vitesse de déformation élevée qui diminue avec le temps. On a trouvé que les vitesses de fluage continuent à diminuer même après plus de trois ans d'essais. On a obtenu une relation empirique entre la déformation des piliers, la contrainte, la température et le temps, qui s'exprime ainsi:

$$\dot{\varepsilon} = 0.39 \cdot 10^{-37}\, T^{9.5}\, \sigma^{3.0}\, t^{-0.70},$$

$$\varepsilon = 1.30 \cdot 10^{-37}\, T^{9.5}\, \sigma^{3.0}\, t^{0.30},$$

avec $\dot{\varepsilon}$ = vitesse de déformation (in./in./h), ε = déformation cumulée (in./in.), T = température absolue (°K), σ = contrainte moyenne dans le pilier (psi), t = temps (h).

A titre de comparaison, on a fait des essais sur modèles réduits avec des échantillons de sel gemme stratifié et de sel de dôme, provenant de six mines des États Unis, et de la structure anticlinale de la mine de sel Asse II dans le nord-est de l'Allemagne. En général, la déformation des différents types de sel à la température ambiante et aux températures élevées était similaire bien que l'on ait observé des variations des vitesses de déformation.

On a observé aussi par des essais sur modèles réduits que les vitesses de déformation sont augmentés considérablement lorsque les cavités contiennent des lits minces de schistes aux contacts du mur et du toit. Les schistes réduisent le frottement; les contraintes de confinement effectives dans le toit et le mur ne sont pas transmises dans les piliers; ainsi, dans ces conditions, les piliers sont moins résistants qu'en l'absence d'intercalation de schiste au sommet et à la base des piliers.

I. Introduction

1. Ultimate Disposal of High-Level Radioactive Wastes in Salt Deposits

Chemical reprocessing of power reactor fuel produces a chemically complex and hazardous effluent which cannot be handled by conventional waste-disposal methods. Special methods of disposal are required to contain these wastes for millenniums, thus preventing the escape of fission products to the biological environment. The most promising method of disposal of high-level, heat-generating, power reactor wastes is the conversion of liquid wastes to solids, followed by the ultimate disposal of the solids in a salt mine[1, 2, 3]. There are several reasons for preferring rock salt for the disposal of radioactive waste, including its availability, geographic distribution, thermal conductivity, and low cost of mining[4]; however, its principal advantage is its characteristic nature of deforming plastically under relatively low stresses and temperatures, which, in turn, accounts for its impermeability. Rock salt deposits, thus, are essentially free of the myriad of fractures that are present in most other rocks and which generally are the principal paths of circulating groundwater. Ironically, this same characteristic of plasticity may also create structural integrity problems in salt mines, especially at elevated temperatures.

It is a well-known fact that salt under certain conditions deforms plastically. The salt dome deposits in the Gulf Coastal area are examples of the natural plastic deformation of halite. Here, enormous quantities of salt have been forced up toward the surface in the form of cylindrical plugs from deep underlying horizontal beds. Flowage of rock salt is also visibly demonstrated in salt mines. Almost complete closure of some of the older drifts and tunnels has occurred in a number of European salt mines that have been worked for several hundred years[5]. At Lyons, Kansas, Dellwig[6] has reported measurable and even visible flowage as early as 30 days after opening new rooms in a salt mine. Heat generated through the decay of fission products will result in a temperature rise in the salt adjacent to cavities used for radioactive waste storage. This greatly affects mine stability, since heating causes a marked increase in the rate of flow of salt. It is, therefore, evident that, in order to properly design excavation cavities in natural salt deposits that will be mined primarily for radioactive waste storage and/or to determine the amounts and locations of wastes that may be stored in abandoned salt mines, it is necessary to be able to predict the effect on mine stability of (1) the supporting-pillar stresses that are a result of the superincumbent earth strata and (2) elevated temperatures that are produced by radioactive decay of the fission products in the waste.

2. Demonstration Disposal of High-Level Radioactive Solids in Salt

The work discussed in this report is an integral part of Project Salt Vault, a demonstration to test the practicallity of high-level radioactive solids disposal in a salt mine. This program, which was initiated in 1962 and is currently nearing completion, has as its principal engineering and scientific objectives (1) the determination of the effects of temperature on the deformation of rock salt, (2) the demonstration of waste-handling equipment and techniques on the land surface as well as in the mine, (3) the determination of the gross effects, if any, of radiation up to 10^9 rad on salt that is heated up to 200^0C, and (4) the determination of any radiolytic production of chlorine[7, 8, 9, 10].

Project Salt Vault has been funded by the Division of Reactor Development of the Atomic Energy Commission. Both the laboratory and field studies that are associated with the project are being carried out under the direction of the Radio-

active Waste Disposal Section of the Health Physics Division at the Oak Ridge National Laboratory. The site of the field demonstration is the Carey salt mine, Lyons, Kansas. Significant quantities of high-level radioactive wastes that would be suitable for storage in salt were not available for this study; thus, irradiated fuel elements were used to simulate solidified high-level wastes. Fourteen irradiated fuel assemblies that were contained in seven cans from the Engineering Test Reactor (ETR) at the Reactor Test Station in Idaho comprised the simulated waste load. In general, the demonstration tests consisted of placing these seven cans in a circular array of holes (one center hole with six peripherally located ones on 5-ft centers) in the floor of a specially excavated portion of the mine. By exchanging the fuel assemblies at the mine for newly irradiated ones at intervals of about 6 months during the period of November 1965 to June 1967, the desired radiation dose and temperature of the salt were attained. In addition to this, an identical array but without fuel assemblies and containing electrical heaters for raising the temperature of the salt was employed to differentiate the effect of heat on the salt from the combined effect of radiation and heat that was evaluated in the fuel assembly array. A second radioactive array was located in the original mine floor where the salt section contains more shale and anhydrite than in the newly mined area. Finally, a single rib-type pillar was heated to provide additional data on the deformation of salt under actual mine conditions at elevated temperatures[7].

A generalized and simplified sketch of the waste-disposal operation at the mine is shown in Fig. 1. The fuel assemblies, which are canned at the Reactor Test Station in Idaho, are shipped via truck to the mine in a specially designed cask. At the charging shaft, the cask containing the cans is raised to a vertical position and the cans are lowered approximately 1000 ft through the cased vertical shaft to the mine excavation below. A specially designed transporter is then used to haul the cans to the test rooms and to place them in the storage holes in the floor. In order to place the fuel assemblies in the purest section of salt, the new mining level was made 14 1/2 ft above the existing mine floor (see Fig. 1).

The Lyons Mine of The Carey Salt Company is located in Rice County, Kansas, near the city of Lyons. The mine was opened in 1890 and closed in 1948. During this period, approximately 100 acres were mined out. The salt was mined by the room-and-pillar method, with salt extraction varying from about 60 to 65%. The floor of the mine lies a little over 1000 ft below the land surface, which is about 1700 ft above sea level.

The Hutchinson Salt Member of the Wellington Formation underlies central and southcentral Kansas (including Rice County) and extends southward into Oklahoma. The member is an integral part of the gently westward-dipping Permian-Pennsylvanian sedimentary rocks that underlie much of Kansas and crop out in the eastern one-third of the state. The salt is not present along this outcrop, probably because it has been dissolved by groundwater and surface water; however, it is present down the dip to the west. The eastern edge of the salt body lies approximately 400 ft below the land surface, but near its western edge in Kansas it is found at a depth of more than 1500 ft. Thickness of the unit range up to as much as 400 ft in Kansas. In general, the Hutchinson consists of a complex mixture of salt, anhydrite, and shale, with salt being the predominant fraction throughout most of its extent in Kansas[11, 12].

At the Lyons Mine, the Hutchinson Salt Member consists of about 300 ft of nearly flat-lying beds of salt, shale, and anhydrite, with salt comprising about 60% of the sequence. The mine was operated in the lower part of the member. Within the mined unit, 1- to 6-in. layers of relatively pure sodium chloride are separated by clay and shale laminae that are usually less than 1 mm in thickness.

These laminae constitute the major impurity in the salt and are characteristic of most bedded salt deposits. Shale beds, several inches in thickness and separated by about 15 to 18 ft of salt, lie above and below the mined unit and thus limit the vertical extent of mining. The mine floor was usually cut within a few inches of the underlying shale bed, while the roof is normally several feet below the over-

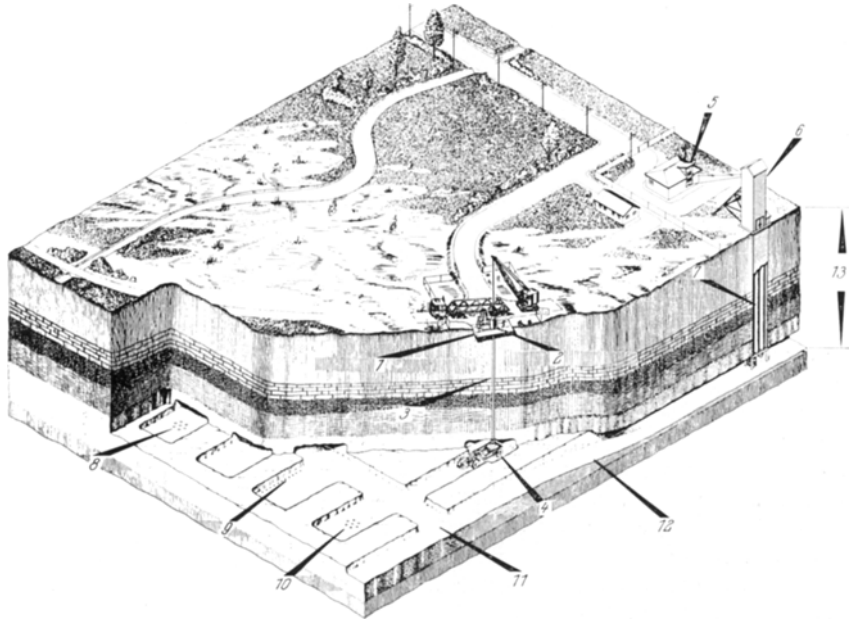

Fig. 1. Demonstration of radioactive solids disposal in salt

1 hoist and work platform; *2* surface waste carrier; *3* waste charging shaft; *4* waste disposal carrier; *5* hoist house; *6* headframe; *7* main shaft; *8* non-radioactive array; *9* pillar heaters; *10* fuel assembly array; *11* new mining level 14 1/2 ft above existing mine floor; *12* ramp to new mine level; *13* existing mine level 1024 ft

Blockbild einer Anlage zur Beseitigung radioaktiver Abfälle in Salz

1 Förderanlage und Arbeitsplattform; *2* obertägiger Abfallbehälter; *3* Ladeschacht; *4* Abfallbehälter; *5* Förderhaus; *6* Schachtgerüst; *7* Hauptschacht; *8* nicht radioaktives Material; *9* Pfeiler-Erhitzer; *10* Treibstoffvorrat; *11* neue Grubensohle, 5 m über der vorhandenen Abbausohle; *12* Rampe zur neuen Grubensohle; *13* bestehende Abbausohle 3,3 m

Illustration du reject des déchets solides dans le sel

lying shale bed. The least contaminated salt, and thus the source of most of the production in the mine, lies in a 9-ft-thick section that extends from the top of the shale below the floor upwards to a thin shale parting, approximately 1/16 in. thick. Another prominent shale parting lies about 3 1/2 ft above the 9-ft roof.

The newly mined demonstration test area lies at a level of about 14 1/2 ft above the pre-existing mine floor and extends upward a distance of about 15 1/2 ft to a thin shale parting at the roof (see Fig. 1). The floor of the newly mined area is comprised predominantly of rock salt, while a thin shale parting marks the roof. A prominent shale bed that varies from a few inches to more than 1 ft in thickness lies approximately 2 1/2 ft above the floor. Two easily distinguishable shale beds that are about 1/8 in. to 1/4 in. in thickness are also observed in the

test area at distances of about 12 ft and 12 1/2 ft above the floor. The salt in the excavation area contains numerous blebs of polyhalite that are commonly concentrated along bedding, giving the salt a banded appearance.

II. Preliminary Investigations

1. Sample Preparation and Test Procedure

To simulate pillar, roof, and floor conditions that would exist in mined cavities in rock salt, sample specimens were fabricated to represent scale models of salt pillars and their surrounding rooms. The test specimens used in this work were cylindrical in shape, with a portion of the center ground out to form the pillar and surrounding rooms. By "epoxying" steel rings around the ends of the samples, effective confining pressure was applied to the roof and floor portions of the models when they were loaded. Constant uniaxial loads were applied to the models by hydraulic compression testers having capacities up to 300 000 lb. Cavity closure was measured by mounting two dial gauges 180° apart on the rings (see Fig. 2). All tests were conducted in a controlled-temperature room, equipped with automatic dehumidifiers to prevent condensation on the samples during extremely damp periods. Elevated temperature tests were performed with the specimens inside a cylindrical heating jacket and with barrier heaters on top and bottom between the specimen and the platens.

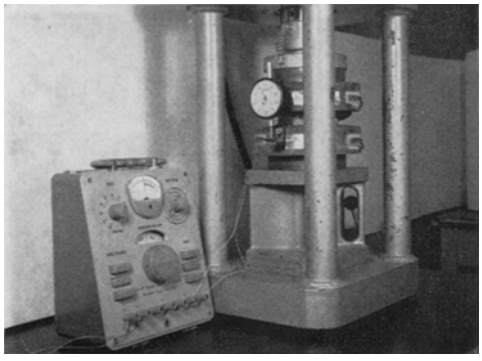

Fig. 2. Pillar model in compression machine
Pfeilermodell in der Materialpresse
Modèle d'un pilier dans la machine de compression

Most tests were performed on model pillars fabricated from 5-11-/16-in.-diam cores of rock salt taken in the mine of The Carey Salt Company, Lyons, Kansas. Similar cores for model tests were recovered from sample cubes of salt, measuring 1 to 2 ft on a side, taken from rock salt mines at Hutchinson, Kansas; Retsof, New York; Detroit, Michigan; Grand Saline, Texas; Cote Blanche, Louisiana; and Asse, Germany. In addition, a few rectangular-shaped models were cut from some of the sample blocks, and, in one case, a 11-1/2-in.-diam core was taken for model testing. Sheet Teflon greased with a mixture of silicon grease and graphite was inserted between the tops and bottoms of the samples and the platens of the compression machines to reduce the friction between the salt and the platens to an insignificant amount. The importance of eliminating the friction between the salt specimens and the test machine platens in ascertaining a true measure of the laboratory deformation of rock salt has been investigated by others[13, 14].

Most tests were conducted at temperatures of 22.5°, 60°, 100°, and 200°C for axial loads of 2000, 4000, 6000, 8000, and 10 000 psi. In addition, a few special tests were conducted on salt samples at loads as high as 15 000 psi. Duration of the tests varied from a few minutes for those specimens where the deformation rate was exceedingly fast to a single case where the sample was allowed to deform over a period of about 3 1/3 years. The most common test time duration varied between about 500 and 1000 hr. For certain temperature and load combinations,

duplicate or triplicate tests were run in order to obtain an approximate measure of variation from sample to sample. About 110 pillar models were tested in these studies.

2. Simulation of Mine Pillars in Scale Models

The deformation characteristics of rock are an extremely important consideration in the simulation of mine conditions in scale-model tests. For example, to determine the stability of mine pillars composed of plastic materials like rock salt, it is absolutely necessary to simulate in the models, not only the mine pillar but also the roof and floor conditions. However, for brittle rocks like dolomite, the roof and floor apparently do not affect greatly the deformation of the pillar.

This has been illustrated in uniaxial tests of model mine pillars of rock salt and dolomite. In both cases, the models were fabricated from 5-11/16-in.-diam cores. After cutting the cores to a lenght of 5 in., a portion of the center of the specimens was ground out as described earlier to form the pillar (1 in. high by 4 in. in diameter) and the surrounding roof and floor. Steel rings were then "epoxied" to the top and bottom portion of the samples to restrain laterally the rock in the roof and floor (as would be the case in actual mine workings). Wire strain gauges were used to determine radial stress on the rings. As seen in Fig. 2, three wire gauges are attached at equidistant locations to the outside portion of each ring. Upon the application of axial stress, the deformation of the steel rings is measured by the strain indicator. For rock salt samples tested at room temperatures, it was found that the radial stress exerted on the rings increased with increasing axial loads up to approximately 75 % (11 250 psi) of the axial load at 15 000 psi (see Fig. 3). However, for the dolomite samples, it was observed that the radial stress did not exceed about 5 % of the axial stress of the pillar load, even at loads as high as 23 000 psi. These data indicate that, for materials that deform plastically like rock salt, actual mine conditions are simulated best when the roof and floor portions of the models are constrained laterally. This allows confining stress in the roof and floor to be transmitted into the pillar (at least for samples having a width-to-height ratio of 4), thereby making the pillar stronger. For dolomite, the relatively small values of radial stress measured on the confining rings of the models indicate that the roof and floor have less influence on the strength of the pillars; and, thus, the simulation of the roof and floor in models used to define mine pillar deformation in rocks of this type are not as critical as for rocks that deform plastically under the same conditions.

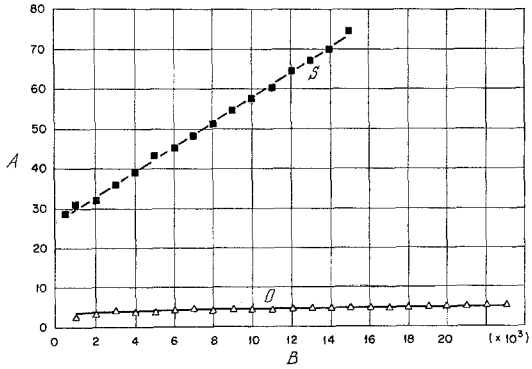

Fig. 3. Radial stress in rock salt and dolomite pillar models

A Radial stress (expressed as percent of axial stress); *B* axial stress (psi); *S* salt (stress rate 33 psi/min); *D* dolomite (stress rate 1000 psi/min)

Radialspannung in Steinsalz- und Dolomit-Pfeilermodellen

A Radialspannung (dargestellt in Prozent der Achsialspannung); *B* Achsialspannung (psi); *S* Salz (Belastungsgeschwindigkeit 33 psi/min); *D* Dolomit (Belastungsgeschwindigkeit 1000 psi/min)

Contrainte radiale dans le sel gemme et dans des modèles de pilier en dolomie

3. Size of Model Specimens

The scaling of mine works to a convenient size for laboratory testing is a matter of great concern in model studies of rock deformation, since all geologic features may not be adequately represented in scaled-down laboratory specimens. Perhaps the most important scaling considerations in regard to the salt mine structures are the size of the test specimens with respect to the grain size of the rock salt and the amount of salt above and below the mine pillars.

To evaluate the effects of various salt thicknesses in the roof and floor of test models, several samples were tested having the same pillar dimensions of 4 in. in diameter by 1 in. in height, but with different thicknesses of salt (7/8, 2, 3, and 4 in.) above and below the pillar. In Fig. 4, which shows pillar deformation with

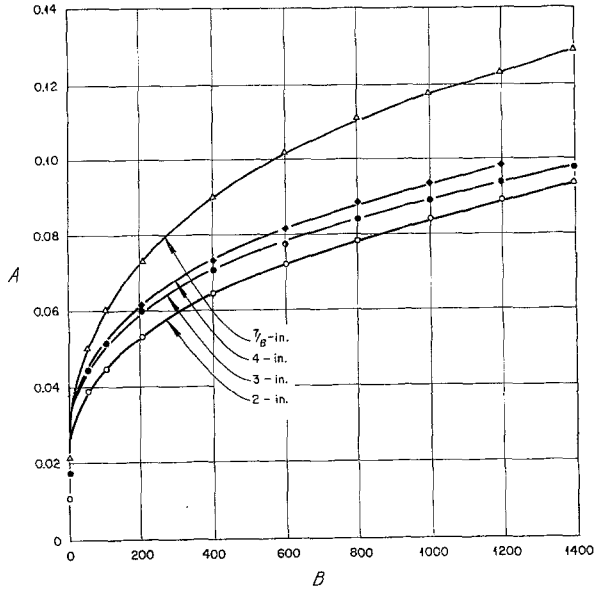

Fig. 4. Deformation of pillar models at 22.5°C and 6000 psi with 7/8, 2, 3, and 4 in. of salt in the roof and floor

A Vertical shortening of pillars (in./in.); *B* time (hr); 7/8-in., 4-in., 3-in., 2-in. = thickness of roof and floor

Verformung von Pfeilermodellen bei 22,5°C und 6000 psi mit 7/8, 2, 3 und 4 Zoll Salz in Firste und Sohle

A Vertikale Verkürzung der Pfeiler (in./in.); *B* Zeit (h); 7/8-in. 4-in., 3-in., 2-in. = Dicke von Firste und Sohle in Zoll

Déformation de modèles de pilier à 22,5°C et 6000 psi avec 7/8, 2, 3 et 4 in. épaisseur du sel sur le mur et sur le toit

time, it is observed that there is little difference in the deformation curves for the samples with 2 in. or more of salt above and below the pillar; however, for the specimen having only a 7/8-in. layer of salt in the roof and floor, the amount and rate of deformation is markedly greater. It is concluded from these data, along with the measured values of radial stress in the roof and floor of model salt pillars as discussed above, that about two times as much or more thickness of salt should lie above and below any given pillar height to approximate the true strength of actual mine pillars.

In addition to the tests discussed above, one specimen having dimensions twice that of the "standard model specimen", that is, an 8-in.-diam pillar having a 2-in. height and a roof and floor thickness of 4 in., was tested at a load of 4000 psi at 22.5°C. The deformation curve for this sample is essentially the same as that for the smaller "standard model" for the same type of rock salt. It is thus concluded that a 5-11/16-in.-diam core of rock salt, that is 5 in. in length, and which is ground out in the center for a 4-in.-diam and 1-in.-high pillar, and, therefore, contains 2 in. of salt in the roof and floor above and below the pillar, adequately simulates mine conditions where the pillar, roof, and floor are essentially all rock salt.

III. Results of Model Pillar Tests

1. General

In order to obtain data on the deformation of rock salt under temperature and pressure conditions that would be expected in an actual disposal operation, a series of model pillars, fabricated from rock salt in the Lyons, Kansas, Mine, were tested at all combinations of axial loads of 2000, 4000, 6000, 8000, and 10 000 psi and temperatures of 22.5°, 60°, 100°, and 200°C. In addition, data on the effects of shale partings and pillar shapes on the deformation of rock salt, which must also be considered in an actual disposal operation, have been obtained from model tests. These data along with field data from the Lyons Mine form the basis for predicting pillar behavior in salt cavities used for the disposal of radioactive wastes. Since the occurrence of rock salt in the United States is rather widespread, it is conceivable that many sites could be used for waste-disposal operations. In order to make gross comparisons of the deformation of salt from one mine to another, model pillars, fabricated from rock salt from five other mines in the United States and one German mine, were tested at temperatures of 22.5° and 100°C and for axial load of 4000 psi. For the following tests, the observed deformations are for salt samples from the Lyons, Kansas, Mine unless otherwise stated.

2. Effect of Load

Fig. 5 shows deformation curves for model pillars of rock salt that have been tested at various temperatures and stresses. These curves all show some similarities even though the stress for each curve is different. For each curve there is initially a high rate of deformation that decreases with time. This decrease in deformation rates is shown to continue out to 300 hr. However, in longer duration model tests, it has been observed that rates continue to decrease even after more than 29 000 hr or 3 1/3 years. It should be added here, too, that this is in agreement with measurements that have been made in salt mines which show that deformation rates are still decreasing with time in openings up to 12 years old[15]. In the figure it is also observed that the deformation of the pillars increased markedly with higher stresses. For the 4000-psi and 22.5°C model the total deformation was about 0.025 in. after 300 hr. Since the pillar was only 1 in. high before deformation, the pillar deformation is about 2 1/2 %. It is also noted that for the sample tested at 6000 psi and 22.5°C the deformation is approximately 0.065 of an inch or 6 1/2 %.

3. Effect of Temperature

Perhaps even more significant than the increased pillar deformation with higher stress is the greatly accelerated deformation at elevated temperatures. In all cases, it is noted that, in general, there is initially a high creep rate that decreases with

time, as in the case with models tested at room temperature. For the tests at 6000 psi it is observed that the effect on pillar shortening by raising the temperature to 60° C is not nearly so pronounced as at 100° C. At the latter temperature the pillar had deformed 35% after about 230 hr, while the deformation at 60° C was less than 20% during the same period of time. In general, cavity closure is complete after about 0.5 to 0.6 in. (50 to 60%) of pillar shortening in models

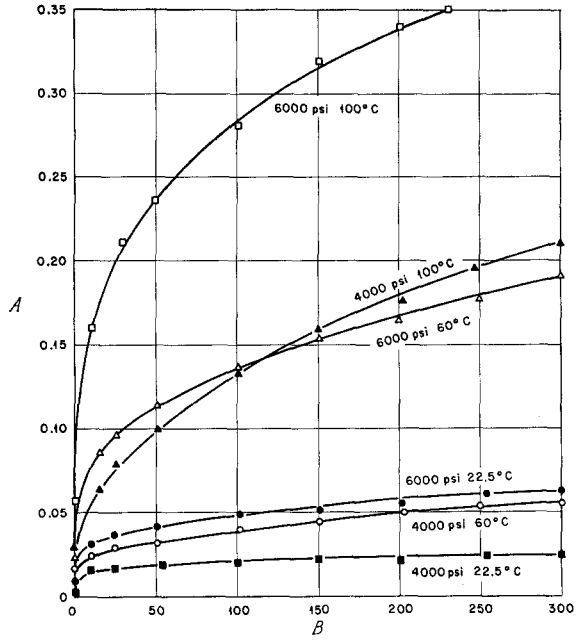

Fig. 5. Deformation of pillar models at various temperatures and pressures
A Vertical shortening of pillars (in./in.); *B* time (hr)

Verformung von Pfeilermodellen bei verschiedenen Temperaturen und Drücken
A Vertikale Verkürzung der Pfeiler (in./in.); *B* Zeit (h)

Déformation de modèles de pilier à différentes températures et pressions

deformed at elevated temperatures. This is due to the lateral flowage of salt into the room opening from the pillar, as well as more or less vertical movement into the opening from the roof and floor, and will be discussed in more detail later.

Salt pillars subjected to elevated temperatures apparently behave like pillars under higher stresses. It is of interest that the deformational behavior of the salt pillar tested at 4000 psi at 60° C is approximately the same as the behavior of the sample tested at 6000 psi and 22.5° C. Also the curve for the 4000 psi model at 100° C is similar to the behavior of the 6000-psi sample at 60° C. This strongly suggests that the net effect of elevating the temperature is essentially the same as that of increasing the pillar stress.

4. Effect of Temperature Elevation After Initial Loading

The general effect of heat on the deformation of rock salt has been discussed above. In these tests, which were carried out to establish empirical relations between temperature, pressure, and time, the samples were first heated and then loaded. However, under actual disposal conditions, the mine pillar would be loaded

first and then the salt would be heated as the rooms are filled with waste. To define pillar deformation under the latter conditions, a model specimen was loaded to 4000 psi at room temperature of 22.5°C for about 800 hr, and then the temperature was increased to 100°C. In the case of both the initial loading and the elevation of the temperature, it is observed in Fig. 6 that the deformation curve rises

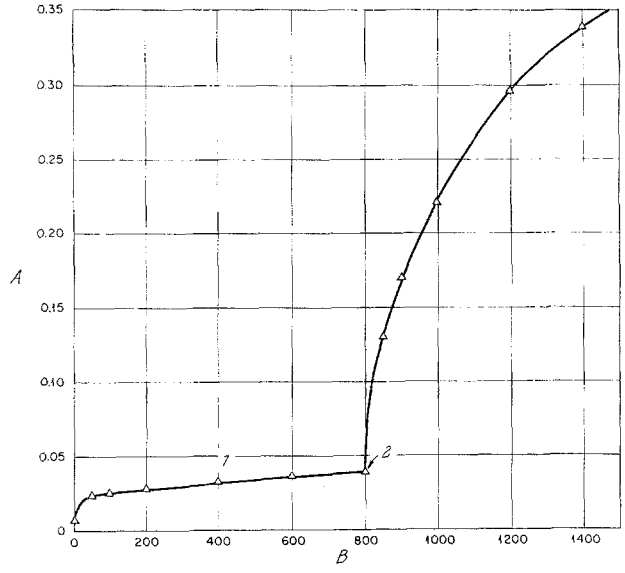

Fig. 6. Deformation of pillar model at 4000 psi and 22.5°C and 100°C
A Vertical shortening of pillars (in./in.); *B* time (hr); *1* temperature at 22.5°C; *2* temperature increased to 100°C

Verformung eines Pfeilermodells bei 4000 psi und 22,5°C
A Vertikale Verkürzung der Pfeiler (in./in.); *B* Zeit (h); *1* Temperatur 22,5°C; 2 Temperaturzunahme auf 100°C

Déformation d'un modèle de pilier à 4000 psi et à 22,5°C et 100°C

sharply initially and then proceeds to rise but at a decreasing rate; however, in the latter case, the total deformation is significantly greater. It is also of interest that, upon the application of heat (the temperature of the salt was raised from 22.5° to 100°C over a period of about 4 hr), there was a corresponding increase in the load on the sample. This increase of load, which was due undoubtedly to the thermal expansion of the salt, attained a peak value of 4640 psi (a 16 % increase) after the salt had reached a temperature of about 80° C or approximately 2 hr after the initial temperature rise. The linear coefficient of the thermal expansion of salt is about 40×10^{-6}. Thus, for a temperature rise of about 77.5°C, the linear expansion for a 5-in.-high salt cylinder would be about 0.0155 in. Furthermore, since four-fifths of the length of the model salt cylinder was confined by steel rings, which reduced the expansion in a radial direction, it is apparent that the vertical expansion of the salt specimen would be somewhat greater than the linear expansion value. (The volumetric or cubic expansion of salt is approximately three times the linear expansion, since sodium chloride is isometric.) It is not likely that the increase in load was due to any increase in the temperature of the hydraulic fluid which drives the ram in the test machine, since 2-in.-thick blocks of a solid insulation material (Transite) were placed between the heated specimen and the

platens of the test device. Thus, no significant amount of heat would be expected to reach the hydraulic fluid for the 4-hr period of the temperature rise. It is also significant that at the time the salt temperature had reached its maximum value of 100°C the load had decreased to the static value of 4000 psi. This test shows that some increase in the load on salt pillars will occur with a significant rise in temperature; however, because of the accelerated flow of salt at elevated temperatures, the load is rather quickly relieved. Since the temperature rise in the salt in an actual mine disposal facility will rise very slowly (probably over periods of many months to years), it is difficult to state precisely, based on laboratory test of pillar models that are uniformly heated within a few hours, the nature of the increase in pillar loading and the relieving of this excess load through salt flow.

5. Effect of Shale Partings

Even though some salt deposits, such as salt domes, are essentially free of other intercalated rocks, most bedded deposits contain lithologic discontinuities of dolomite, shale, anhydrite, and other materials. For instance, the 300-ft-thick salt sequence at Lyons, Kansas, is only about 60% NaCl with the other 40% being mostly shale and anhydrite. In many cases these "other" materials may form a part of the roof, floor, or even the pillars in a mine and thus enter into the deformation of the openings. In Fig. 7 the occurrence of thin shale beds in salt mines is depicted. In the one case, thin shales are shown at the top and bottom of a mine pillar as separating the pillar from the floor and ceiling. Shale beds such as this are common in bedded salt, and in many cases the salt is mined or falls to these partings, since they serve as effective friction reducers. In the second case, a single shale bed occurs in the center of the pillar, with salt continuing uninterrupted from the pillar into the area above and below. The presence of these partings, even though they are quite thin, can have a significant effect on the rate of cavity deformation, depending on whether the shale is at the top and bottom of the pillar or in the center of it. This is shown in Fig. 8, where deformation curves are presented for model salt pillars that have been deformed (a) without any simulated shale partings, (b) with simulated shale partings as the top and bottom of a pillar, and (c) with a simulated shale parting in the center of the pillar. Thin sheets of Teflon lubricated with grease and graphite serve as friction reducers and thus simulate shale partings. Analysis of data and observations from the Kansas mines indicates that the shale partings do have lubricating effect, but it does not appear that they have so marked an effect as do the Teflon sheets. Therefore, the actual effects to be expected in a mine would lie somewhere between the two extremes, shown in Fig. 8. For the model having no simulated shale partings, and for the model where the shale parting is in the center of the pillar, the deformational curves are almost identical, both showing about 0.03 in. or 3% deformation after 140 hr of testing. However, for the model with friction reducers at the top and bottom of the pillar, the deformation proceeds initially at a very fast rate before beginning to decrease with time. The model appears to then deform

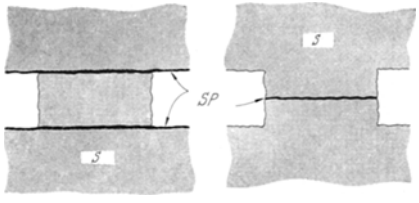

Fig. 7. Sketch showing lithologic discontinuities in salt mines
S salt; *SP* shale partings

Skizze lithologischer Diskontinuitäten in Salzbergwerken
S Salz; *SP* Schieferton-Ablösungen

Schéma des intercalations schisteuses dans les mines de sel

at a constant rate for a short time and then at an increasing rate that results in sudden failure after less that 130 hr. It is also of interest that for models with no simulated shale partings, sudden or catastrophic pillar failure could not be induced even under stresses as high as 150 000 psi.

Excavations in bedded salt deposits may sometimes contain shale beds at only the top or at only the bottom of pillars. In Fig. 9 the behavior of model pillars with natural shale beds at the tops of the pillars is compared to the deformation of a model having a simulated shale parting and a model without shale partings. All of the

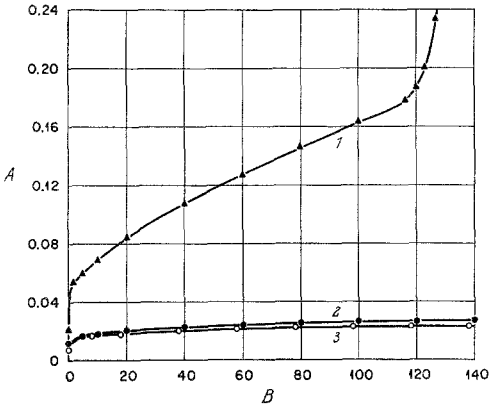

Fig. 8

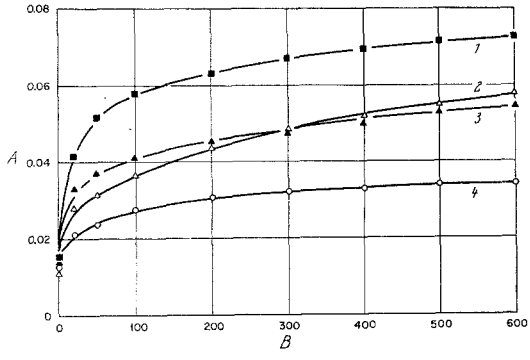

Fig. 9

Fig. 8. Deformation of pillar models at 4000 psi and 22.5° C and with and without simulated shale partings

A Vertical shortening of pillars (in./in.); *B* time (hr); *1* with friction reducer at floor and ceiling; *2* without friction reducer; *3* with friction reducer at center of pillar

Verformung von Pfeilermodellen bei 4000 psi und 22,5° C mit und ohne nachgebildeten Schieferablösungen

A Vertikale Verkürzung der Pfeiler (in./in.); *B* Zeit (h); *1* mit Reibungsverminderung an Firste und Sohle; *2* ohne Reibungsverminderung; *3* mit Reibungsverminderung in der Mitte des Trägers

Déformation de modèles de pilier à 4000 psi et 22,5° C avec et sans intercalation de schistes

Fig. 9. Deformation of pillar models at 4000 psi and 22.5° C and with natural and simulated shale partings and without shale partings.

A Vertical shortening of pillars (in./in.); *B* time (hr); *1* natural shale roof; *2* simulated shale parting; *3* natural shale parting; *4* without shale parting

Verformungen von Pfeilermodellen bei 4000 psi und 22,5° C mit natürlichen und nachgebildeten Schieferablösungen sowie ohne Schieferablösungen

A Vertikale Verkürzung der Pfeiler (in./in.); *B* Zeit (h); *1* natürliche Schiefertonfirste; *2* nachgebildete Schieferablösung; *3* natürliche Schieferablösung; *4* ohne Schieferablösung

Déformation de modèles de pilier à 4000 psi avec intercalations schisteuses naturelles et simulées et sans intercalations

specimens with shale partings show, as expected, greater deformation than the sample without shale. For the sample with the Teflon simulated shale parting, the deformation rate is initially slower than the models with the natural shales, but the deformation rates for the latter samples decrease at a more rapid rate than does the sample with the simulated shale. The thickness of the shale parting is

approximately 1/8 in. in the model showing the lower deformation curve, while the remaining one is composed essentially of a shale roof and a rock salt pillar and floor. This difference in thickness of the shale section in the models probably accounts for the variation in deformational behavior.

The accelerated deformation rate of the models, when simulated shale partings occur at the top and bottom of the pillars, apparently results from the more or less independent deformation of the pillar from the roof and floor under these conditions. When there are no partings at the top and bottom of the pillar, or even if the parting is in the center of the pillar, there is an interlocking effect of salt crystals from the pillar to the roof and floor which serves to allow the pillar, roof, and floor to deform more or less as a single unit. However, when partings exist between the pillar and the roof and floor, they serve as effective friction reducers, which consequently allow the pillar to deform more independently of the roof and floor, and horizontal confining pressures in the roof and floor are not transmitted into the pillar.

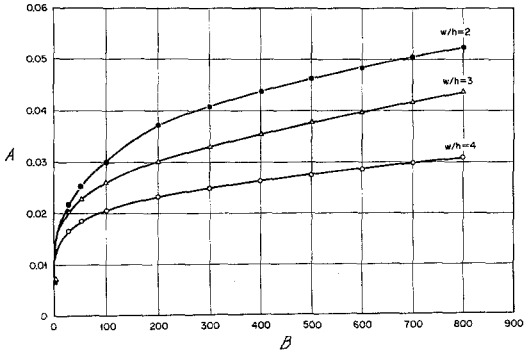

Fig. 10. Deformation of pillar models at 4000 psi and 22.5° C and with width-to-height ratios of 2, 3, and 4

A Vertical shortening of pillars (in./in.); *B* time (hr)

Verformung von Pfeilermodellen bei 4000 psi und 22,5° C und Breiten- und Höhen-Verhältnissen von 2, 3 und 4

A Vertikale Verkürzung der Pfeiler (in./in.); *B* Zeit (h)

Déformation de modèles de pilier à 4000 psi et 22,5° C et avec rapports largeur-hauteur de 2, 3 et 4

6. Effect of Pillar Shapes

The width-to-height ratio of salt pillars is an important consideration in predicting mine closure. This is illustrated in Fig. 10 which shows pillar deformation with time for models having width-(diameter-)to-height ratios of 2, 3, and 4. All pillars were originally 1 in. in height, while their widths were 2, 3, and 4 in. From the curves it is seen that pillar shortening proceeds at a faster rate with the smaller diameter-to-height models. Thus pillar strength increases with increasing width-to-height (w/h) ratios. For instance, after 800 hr of testing, it is observed that the $w/h = 3$ sample had deformed about 0.0435 in. or approximately 43 % more than the $w/h = 4$ specimen which had deformed only about 0.0305 in. The $w/h = 2$ pillar showed an even greater deformation of 0.0525 in. or 73 % more pillar shortening than the $w/h = 4$ sample after the same period of testing.

In addition to these tests, a few models having rectangular-shaped pillars were deformed. (All previously deformed model pillars were cylindrical in shape.) Tests were conducted on models having overall dimensions of 6.45 by 3.94 in. and with pillar dimensions of 5.01 and 2.51 in. The lengths of the pillars were, therefore, approximately twice their widths, and the salt extraction was about 50 % or roughly the same as that for the cylindrical samples. Under these conditions, significant differences in pillar deformation are apparent when the rectangular-shaped specimens are compared to the cylindrical-shaped specimens with the same horizontal cross-section areas. For a rectangular-shaped specimen and a cylindrical-shaped

specimen tested at 4000 psi and 22.5°C, the rectangular-shaped pillar was found, after 1000 hr, to have deformed about 40 % more than its cylindrical counterpart.

The greater strength of cylindrical pillars to their rectangular counterparts may be explained, in part, by the apparently high concentrations of stress at the corners of the rectangles which lead to spalling of the salt at these locations and, thus, to reductions in the cross-sectional area over which the loads are distributed. Also, it would appear that, as the lengths of rectangular-shaped pillars increase in relation to their widths (for the same cross-sectional area), the pillars will be correspondingly weaker. This is due, presumably, to reductions in the transmission of confining stresses from the roof and floor portions of the specimens to the pillars as would be also the case for round pillars having width-to-height ratios less than 4. It was shown earlier, in the case of specimens having shale partings at the tops and bottoms of the pillars, that when confining stresses are not transmitted into the pillars from the roofs and floors, the pillars are considerably weaker than when confining stresses are effectively transferred into the pillars.

7. Comparisons of Salt from Various Localities

In order to make a general comparison of the deformational behavior of rock salt from various localities in the United States, as well as from European deposits, tests were conducted at 4000 psi and at temperatures of 22.5° and 100°C on model pillars fabricated from salt samples taken in mines at Lyons and Hutchinson, Kansas; Retsof, New York; Detroit, Michigan; Grand Saline, Texas; Cote Blanche, Louisiana; and Asse, Northeast Germany. The Kansas salt is from a bedded deposit of Permian age, while the New York and Michigan salts are bedded and of Silurian age. The Grand Saline and Cote Blanche mines are situated in dome-type deposits. The Asse salt is mined from an anticlinal structure.

For the tests at 22.5°C, shown in Fig. 11, it is observed that the deformation curves for the Lyons, Hutchinson, Michigan, Cote Blanche, and Asse II mine deposits are strikingly similar; however, the Grand Saline mine salt deforms at a slightly greater rate, and the salt from the Retsof mine deforms, at least initially, at an even more accelerated rate.

As seen in Fig. 12 for the 100°C tests, there is a rather wide spread in the deformation associated with the various types of salt. The Lyons, Hutchinson, Cote Blanche, and Grand Saline curves are similar and show the largest amounts of pillar shortening after about 800 hr. The Retsof sample is observed to deform at a markedly slower rate. The curve for the Detroit salt is distinctly different from the others in that the deformation rate is initially slower, but it does not decrease as rapidly with time. Thus it appears from these tests that the total deformation for the Detroit salt will eventually exceed that of the other deposits. The Asse II salt, under these conditions, appears to be stronger than the others.

The reasons for the differences in the behavior of the salts from the various localities as shown in these tests are not fully understood. The depths of the mines do not vary greatly, most being about 1000 ft deep; thus the overburden loads that the salts have been subjected to in Recent geologic time and the resulting prestrained conditions (before laboratory testing) of the samples would appear to be roughly the same. All of the salts are relatively low in insolubles, varying from 0.78 % (Detroit) to 2.27 % by weight (Hutchinson); therefore, the differences in deformation behavior would not appear to be explained by the presence of at least large quantities of impurities in some deposits. However, the Retsof and Asse II salts, which appear to deform after the initial deformation at a slower rate than the other salts, contain about twice the quantity of water insolubles than do the

samples from the other localities with the exception of the Hutchinson salt. Using X-ray diffraction techniques, it was found that anhydrite was the principal water insoluble impurity for all samples except the Asse II salt which contained polyhalite as its major impurity.

There do not appear to be any consistent differences in behavior related solely to the three structural types of deposits; namely, domal, anticlinal, or bedded. Differences in grain size may account for some of the variations in deformation; however, all samples are extremely coarse grained with the exception of the Retsof and Asse II salts. The Retsof salt is unique in that there is a pronounced lack of grain intergrowth and the grains are apparently not firmly cemented together; thus the texture of the salt is somewhat friable. This may account for the high initial

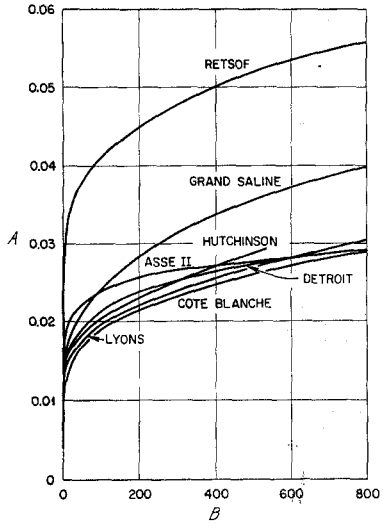

Fig. 11

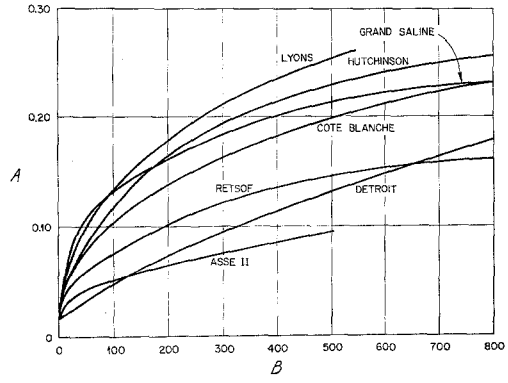

Fig. 12

Fig. 11. Deformation of pillar models from various localities at 4000 psi and 22.5°C
A Vertical shortening of pillar (in./in.); *B* time (hr)

Verformung von Pfeilermodellen von verschiedenen Örtlichkeiten bei 4000 psi und 22,5°C
A Vertikale Verkürzung der Pfeiler (in./in.); *B* Zeit (h)

Déformation de modèles de pilier de différentes localités à 4000 psi et 22,5°C

Fig. 12. Deformation of pillar models from various localities at 4000 psi and 100°C
A Vertical shortening of pillars (in./in.); *B* time (hr)

Verformung von Pfeilermodellen von verschiedenen Örtlichkeiten bei 4000 psi und 100°C
A Vertikale Verkürzung der Pfeiler (in./in.); *B* Zeit (h)

Déformation de modèles de pilier de différentes localités à 4000 psi et 100°C

deformation rate of the Retsof salt, since some compaction and reorientation of grains would be expected to occur when the salt is loaded initially. Perhaps the thermal expansion of the salt was instrumental in reducing the intergranular voids for the 100°C test, which did not experience the extremely rapid initial deformation as did the sample tested at 22.5°C.

8. Ultimate Strength

The ultimate strength of support systems is of fundamental importance in all underground openings. To determine the ultimate or breaking strength of mine pillars in salt, two models, one having a width-to-height ratio of 3 and the other a width-to-height ratio of 4, were loaded at rates of 33 psi per minute until failure or extensive deformation occurred. The deformation curves for these samples are

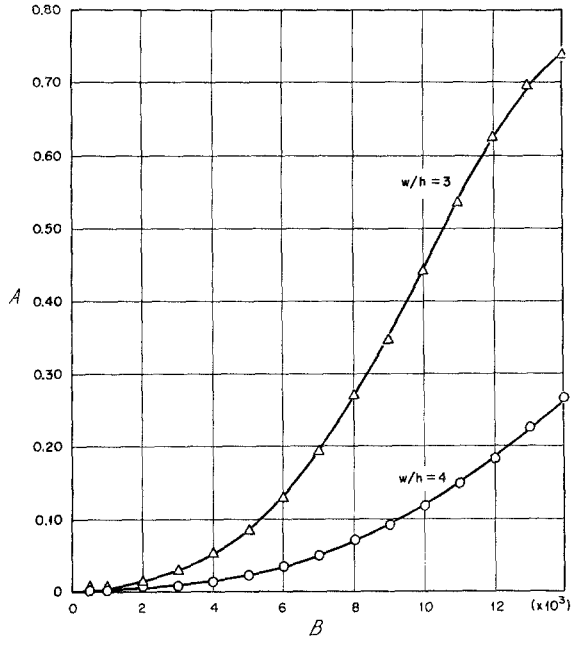

Fig. 13. Ultimate strength of pillar models at 22.5° C and with width-to-height ratios of 3 and 4

A Vertical shortening of pillars (in./in.); *B* axial stress (psi)

Tragkraft von Pfeilermodellen bei 22,5° C und bei Breiten-Höhen-Verhältnissen von 3 und 4

A Vertikale Verkürzung der Pfeiler (in./in.); *B* Achsialspannung (psi)

Résistance à la rupture de modèles de pilier à 22,5° C et avec rapports largeur-hauteur de 3 et 4

shown in Fig. 13. In both cases it is seen that sudden or brittle pillar failure did not occur even for loads as high as 14 000 psi; however, considerably more deformation did occur for the smaller diameter pillar than for the larger one. This verifies the conclusion drawn from other tests, described above, that pillars having a width-to-height ratio of 4 are stronger than those having a width-to-height ratio of 3. Although 100% pillar shortening was not attained for either sample, both were deformed to the extent that accumulation of spall or small pieces of broken salt from the pillars had filled a part of the cavity opening. Thus, the effective pillar diameter for the smaller diameter pillar had increased to the point that it extended almost the entire width of the excavated cavity. The combined effects of pillar shortening and pillar spall in cavity closure are discussed in more detail later; however, it is concluded that the smaller the width-to-height ratio of the pillars (assuming a greater excavation ratio), the greater the amount of pillar shortening prior to complete cavity closure. The results of these tests also suggest that sudden

or brittle pillar failure will not occur in salt pillars having width-to-height ratios of 3 and 4, at loads up to 14 000 psi and perhaps even at any higher loads, although it is recognized that deformation of the pillars through creep of the salt would occur at a very high rate. The ultimate strength or breaking strength of these type pillars thus cannot be determined, since the salt under these conditions will flow very rapidly but will not fail in a brittle manner regardless of the load.

9. Mechanisms of Deformation

Although the exact mechanisms of the deformation within salt pillars are not fully understood, some generalizations as to movement have been formulated through observations of deformed specimens. Fig. 14 shows cross-sectional views of two model pillars that have been cut vertically in half after deformation. Before deformation, the pillars were 4 in. in diameter and 1 in. high. In these specimens an attempt was made to define the principal movement through observing the relation of the pillar and the material above and below it after deformation. The dark horizontal lines seen in the salt specimens are 1/16-in.-diam holes that were bored horizontally through the tops and bottoms of the pillars and filled with colored salt before the specimens were deformed. In the model pillar deformed at 22.5° C, it is seen that the pillar is only slightly more than 4 in. in diameter. However, a considerable amount of loose salt from the outermost portion of the pillar had accumulated in the surrounding cavity opening but was subsequently removed. The cross-sectional view shows that the pillar did not deform independently of the roof and floor but that all three parts of the model entered into the closure of the cavity. Note especially how the roof and floor have flowed into the cavity opening. The most resistance to deformation in the model is believed to be found in the center portion of the pillar (due to confining pressure) and immediately above and below the pillar in the roof and floor. Thus, movement here is at a minimum. This is shown in the photograph by the greater distance between the lines in the center portion of the pillar than at the edge of the pillar. Toward the ouside of the pillar, there is less resistance to deformation; thus, salt from the pillar tends to move horizontally into the opening, while material from above and below also moves in to fill the cavity.

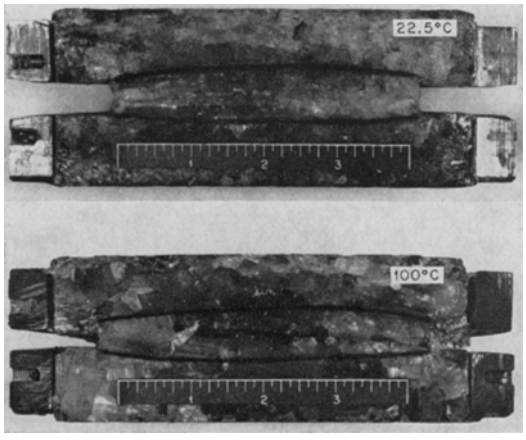

Fig. 14. Photograph of pillar models showing vertical deformation at 22.5° C and 100° C

Pfeilermodelle mit den vertikalen Deformationen bei 22,5° C und 100° C

Photo de modèles de pilier montrant la déformation verticale à 22,5° C et 100° C

In the model pillar deformed at 100° C, the overall deformational pattern is similar to that for the sample tested at room temperature; but, instead of the outermost portion of the pillar deforming through spalling, it stayed intact and deformed more plastically. The pillar diameter in this case increased from 4 in. to 4 1/2 in. as a result of the deformation.

In the preceding figure it is observed that cavity closure is due to the lateral flowage of salt from the pillar into the opening, as well as to the more-or-less ver-

tical movement of salt into the cavity from the roof and floor. In general, this type of deformation prevails at ambient temperature, as well as at elevated temperatures; however, in the case of the former, the effective width of the pillar remains about constant, since the amount of pillar spall approximates the lateral flow of salt from the pillar, while at elevated temperatures there is a progressive increasing of the pillar width with deformation since there is little or no pillar spall and the salt flows en masse. This increase in pillar width, which results in a lower pillar stress, undoubtedly accounts, in part, for the marked decrease in the rate of cavity closure with time, especially when the total deformation exceeds about 50 %. Thus, when the salt is heated, it is apparent that initially there will be a rapid increase in pillar shortening, the rate being dependent, of course, on the temperature and load. Then, as the pillar width increases and the cavity becomes filled, there is another pronounced decrease in the rate of cavity closure which continues until all of the void space is filled with salt from the pillar or from the roof and floor. For the model salt pillars tested at 22.5°C and even for those tested at temperatures of 60°C and at loads no greater than 4000 psi, the deformation proceeds at such a slow rate that it was not possible to observe total cavity closure for the duration of the tests in the laboratory. However, it is presumed that, since there is no effective increase in the pillar width due to pillar spall at ambient temperatures, there would be no decrease in the axial load on the pillar and, thus, no flattening of the deformation curve until the accumulation of salt in the cavity from the pillar spall is sufficient to fill essentially the entire cavity. Pillar spall commonly occurs as thin and somewhat elongated fragments that separate along nearly vertical tension cracks that develop on the pillar walls as a result of the outward flow of salt.

IV. Discussion

1. Relationship of Load, Temperature, and Time

In order to be able to predict the effects of load, temperature, and time on underground openings in salt deposits, empirical equations have been developed that fit the results of the model pillar tests of rock salt from the Lyons, Kansas, Mine having a pillar width-to-height ratio of 4. These equations are expressed as

$$\dot{\varepsilon} = 0.39 \cdot 10^{-37} T^{9.5} \sigma^{3.0} t^{-0.70},$$

$$\varepsilon = 1.30 \cdot 10^{-37} T^{9.5} \sigma^{3.0} t^{0.30},$$

where

$\dot{\varepsilon}$ = strain rate or vertical shortening of pillars (in./in./hr),

ε = cumulative deformation (in./in.) (after 2 min of test time),

T = absolute temperature (°K),

σ = average pillar stress (psi), and

t = time (hr).

To determine the time component in the equation, the cumulative deformation of the complete series of samples tested at temperatures of 22.5°C, 60°C, 100°C, and 200°C, at loads ranging from 2000 to 10 000 psi, were plotted, logarithmically, against time. The data were then fitted by a series of straight line plots after 1 hr, having the slope 0.30. In general, the straight line plots fit the data remarkably well over most of the range of the tests. In these plots cumulative deformation is taken after 2 min of test time. This method of expression eliminates most of the effects of extraneous variation in the rates of deformation from sample to sample.

In an actual mine operation, it is not possible to measure the early deformation phase; thus, the rate of deformation, which is the time derivative of cumulative deformation, is a more important variable than perhaps an extremely precise measure of the total cumulative deformation. Data on cumulative deformation in excess of 0.30 in. per inch were not included, since, at these high values the effects of lateral pillar expansion due to plastic flow, and perhaps even pillar spall, which can only be

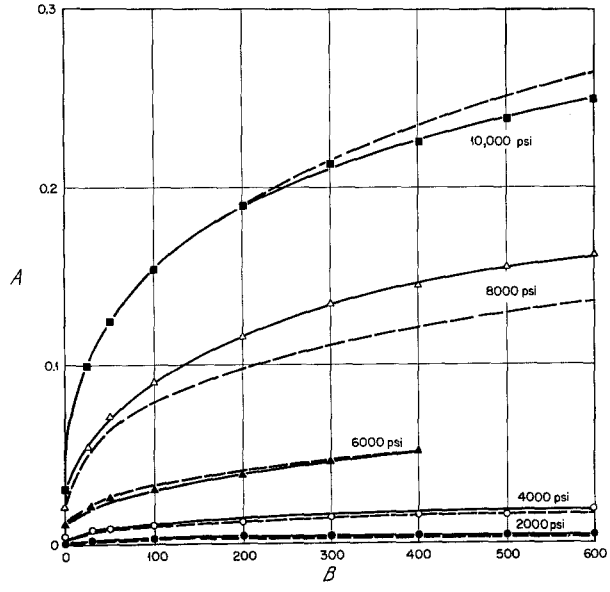

Fig. 15. Comparisons of deformation from tests of pillar models at 22.5° C and from empirical equation

A Vertical shortening of pillars (in./in.) minus first two minutes; *B* time (hr); points are test data; — — — data from empirical equation

Vergleich der Verformung nach Versuchen mit Pfeilermodellen bei 22,5° C und nach empirischen Formeln

A Vertikale Verkürzung der Pfeiler (in./in.) abzüglich der ersten zwei Minuten; *B* Zeit (h); · · · Versuchsdaten; — — — empirische Formeln

Comparaisons des déformations entre les essais sur modèles de pilier à 22,5° C et celles calculées par l'équation empirique

measured qualitatively, influence markedly the deformational behavior of the models. Thus, the deformational behavior of mine pillars above about 30 % of pillar shortening is not predictable with the equations above. In an actual disposal operation, it is planned to backfill the rooms with crushed salt excavated from other parts of the mine as containers of waste are disposed in the mine floors. Under these conditions, it is unlikely that deformation could exceed about 30 % anyway.

The stress function in the equation above was determined by plotting, logarithmically, cumulative deformation for various stresses at a selected period of time. The resulting points for a selected time were then fitted with a straight line having a slope of 3.0. Plots of the several stresses and cumulative deformation at elevated temperatures show about the same average value as that at ambient temperature for the effect of stress on pillar deformation.

To determine the temperature component in the equation, logarithmic plots of cumulative deformation versus temperature for various sample specimens were made and then fitted with a straight line having a slope of 9.5. This steep slope or high value for the exponent of temperature indicates that temperature is the single most important parameter that affects cavity closure in salt mines.

Fig. 15 shows comparisons of the actual deformation curves for model specimens and calculated curves for the same conditions of temperature, time, and load, using the equations given above, at a temperature of 22.5°C. It is observed that the calculated curves are similar to the actual ones at 2000, 4000, and 6000 psi; and, even at the higher loads, there is good agreement between the two plots. In general, the calculated curves show a closer similarity to the actual ones at the lower stresses and at the lower temperatures than at the higher loads and temperatures, especially at the upper ends of the curves where deformation is greatest. These deviations at the higher loads and temperatures are believed to be due to the effects of pillar spall and lateral pillar expansion in the heated samples which undoubtedly affect deformation under high load and temperature conditions and which have not been taken into account in the equation.

2. Relationship to Actual Mine Conditions

Since the model pillar specimens of salt from Lyons, Kansas, that were used in the test to develop the equation were essentially all salt and did not contain shale beds or other rocks in the roof, floor, and/or pillars, predictions using the equations are valid, strickly speaking, only for that type salt. However, the closure rates of excavations in bedded, as well as dome, salt deposits that do not contain shale partings or other rock types in critical areas could also be approximated by these equations. The expressions would be expected to be least effective in predicting deformation in mine openings where shale beds occur at both the top and bottom of the pillars. Since the shales serve as effective friction reducers, confining stresses in the roof and floor portions of the mines are not transmitted into the pillars; thus mine pillars under these conditions will deform as if they were simply squeezed between two rigid plates. The strength of actual mine pillars based on the model study would be expected to be perhaps several times less for conditions where shale partings occur at the tops and bottoms of the pillars than where salt continues uninterrupted from the pillars into the roof and floor. Also, the effect on deformation would not be expected to be nearly so pronounced where the shale occurs only at the top or bottom of the pillar. If salt deposits do contain shale partings that cannot be avoided in mining, it is better that the openings be made so that the shales are located in the center part of the pillar. The center of the pillar apparently is a more-or-less neutral plane, and, therefore, shale partings at this location will not influence the rate of deformation; however, as the location of the shales approach the top or bottom of the pillar, they cause an increasingly greater increase in the rate of cavity closure. In general, a similar pattern of deformation occurs for shale beds in the floor and ceiling of salt mines. The nearer the shale parting in the ceiling and/or floor to the pillar, the weaker is the pillar. This is due to the fact that as the thickness of the uninterrupted salt section that lies in the roof and floor above and below the pillar is reduced, there is a corresponding reduction in the confining stress in the roof and floor which can be transmitted into the pillar. When shale partings lie only a few inches above and/or below the pillars in mines, it is common for buckling of the roof and/or heaving of the floor to occur. This type of deformation not only results in a more rapid closure of the mined opening but creates mine safety problems, since ceiling slabs commonly sag to a considerable extent and then fail and fall suddenly.

Even though there are some variations in the creep rates of salt from one mine to another and even within a single mine where such things as impurities, grain size, texture, etc., may cause slight differences in behavior, it seems apparent that the general creep behavior of salt is the same regardless of the origin and/or location of the deposit. The principal difference then is one of the magnitude of the creep rate. (The rate of creep was found to decrease with time in the model tests, and this has also been verified in mine openings that are up to 12 years old.) Furthermore, it is apparent that the most important parameters that effect cavity closure in salt deposits that might be used for the disposal of high-level wastes are not those of location and genetic type of deposit, grain size, impurity content, texture, etc., but include the presence of shale partings at or near the pillar-floor and/or pillar-ceiling contacts, the width-to-height ratios of the pillars, and the effects of temperature, load, and time.

Based on the results of model tests, mine pillars having width-to-height ratios of 2 and 3 will deform approximately 75 to 45 % faster, respectively, than pillars having a width-to-height ratio of 4. For pillars with width-to-height ratios less than 2, it would appear that the rate of deformation will be even greater. It is also apparent that for mine pillars having width-to-height ratios of 3 or 4, catastrophic pillar failure will not occur at ambient temperature, even at loads as high as 14000 psi, which is well beyond the upper limit of loading that would be expected in any salt mine that would be used for the disposal of wastes. Pillars having widths about four times their heights appear to be most common type in the Carey salt mines at Lyons and Hutchinson, Kansas. Also, the widths of the rooms between the pillars at these mines appear to be about one-half the width of the pillars.

It is apparent that the greater the percentage of extraction of salt from underground workings the greater the superincumbent load on the salt remaining in the pillars. Also, in general, the higher the percent of salt extraction, the smaller the width-to-height ratio of the supporting pillars. For these larger cavity openings and slimmer pillars, correspondingly greater floor-to-ceiling convergences will occur in mines prior to complete cavity closure.

Cylindrical-shaped model pillars were used for the tests to develop the empirical equations given above; however, in actuality, mine pillars may be nearly cylindrical to rectangular. For rectangular-shaped pillars in mines having lengths about twice their widths and containing the same cross-sectional area and height as pillars with width-to-height ratios of 4, it is assumed, from model tests, that they will deform about 40 % faster than their cylindrical counterparts. Rectangular-shaped pillars with lengths several times their widths may be used for specially mined excavations in salt used for the disposal of high-level radioactive wastes. However, it is assumed that width-to-height ratios less than 2 would not be used.

3. Relationship to Field Experiments in Project Salt Vault

The principal objectives of the field or mine tests associated with Project Salt Vault were to demonstrate the overall feasibility and safety of disposing high-level wastes in rock salt deposits and to demonstrate the use of waste-handling techniques and equipment. These two objectives were achieved in the recent tests conducted at the Carey salt mine, Lyons, Kansas[16]. In addition, extremely useful data were obtained from the field investigations on the effects of radiation, overburden load, temperature, and shale partings on the behavior of salt under actual operating conditions. Briefly, the principal mine experiments of interest consisted of three separate array tests and a heated pillar test. As seen in Fig. 1 a seven-can fuel assembly array and its nonradioactive counterpart are located in the specially

mined experimental test area. (The two arrays are identical, except the nonradioactive one uses only electrical heat to raise the temperature of the salt, while the radioactive one contains irradiated fuel assemblies to emit radiation and provide decay heat supplemented by electrical heaters.) A second radioactive array (not shown in Fig. 1) is located in the floor of the former mine level in Entry 5 where the salt section contains considerably more shale and anhydrite than in the newly mined experimental area.

The maximum radiation dose to the salt adjacent to the seven-can radioactive fuel assembly array exceeded 5×10^8 rads, and there were no discernible effects observed that might be detrimental to waste disposal operations[16]. (The deformation of salt in and around the nonradioactive array was essentially the same as that of the radioactive one.) Due to the shielding properties of rock salt, the area affected by the radiation is small. For example, the radiation dose drops about 2 orders of magnitude in the first foot of salt around the cans. Furthermore, the dose is reduced essentially to zero at the edge of the pillars in the test rooms which are about 15 ft from the array. Thus, even if detrimental effects, such as a reduction in the strength of rock salt, should occur at even higher doses than those achieved in the field tests, it would have little effect on the salt in the supporting pillars.

As was anticipated from the model tests, the effect of heat on the salt in the array tests, as well as the heated pillar test, caused marked accelerations in the rates of deformation. In the array tests, it was observed that as heat was applied to the salt (peak temperatures of 200°C were attained in the salt in the centers of the arrays) noticeable uplifts occurred in the floors, being greatest at the center points of the arrays. This expansion of the salt in the floors was observed to extend outward and into the edges of the pillars almost immediately after startup but before any temperature rises were recorded in or beneath the pillars. The expansion of salt under the pillars undoubtedly caused higher effective loads on the pillars, since significant increases in the rates of deformation of the pillars were also measured.

In general, the heated pillar tests consisted of heating the floor around the 20-ft-wide by 60-ft-long pillar, with a total of 22 heaters, each having an electrical output of 1.5 kw (see Fig. 1). The peak temperature of the salt under the center of the pillar was about 70°C. Highest temperatures, of course, occurred under the edges of the pillar, near the heaters. As expected, the greatest increase in the rate of deformation occurred where the temperature rise was greatest and the least where the temperature rise was least. Initially, the overall rate of pillar shortening was increased from about 0.2 in. per year to about 2.0 in. per year or by about a factor of 10 as a result of the thermal stress in the salt[16].

Within the demonstration test area, prominent shale partings occur at the ceiling, in the roof at a distance of 2 ft, and within the excavated portions of the experimental area at distances of about 12 ft and 12 1/2 ft above the floor. Also, a thick shale bed occurs about 2 1/2 ft above the floor. As was expected from the model tests, the thick shale bed, as well as the shale partings, at distances of 12 ft and 12 1/2 ft above the floor had no significant effect on the deformation of the pillars; however, the shale partings at the ceiling and in the roof caused some increase in the rate of deformation of the salt. The lateral expansions of the top parts of the pillars (before the start of heating) in the experimental area were observed to be greater than the bottom portions where there is no shale parting between the floor and pillar. Thus, it is concluded that the shale parting at the ceiling served effectively as a friction reducer and thereby caused the upper part of the pillar to deform somewhat independently of the roof. This same phenomenon has been demonstrated in the model tests. Due to the separation of the salt column at

the shale parting lying 2 ft above the ceiling, the vertical convergence of the roof and floor in the experimental area was greater than that observed in the array test area in Entry 5 where shale partings are absent up to distances at least 5 ft above the ceiling. The effect of shale partings that occur in the roof in increasing the rates of deformation in excavations in salt has also been observed in model tests.

V. Conclusions

The most promising geologic environment for the disposal of large quantities of heat-generating, high-level, radioactive waste is subterranean rock salt deposits. To investigate the deformational behavior of rock salt in mined openings, scale models of salt pillars and their surrounding rooms were fabricated and tested under conditions that might be expected in actual operations. Laboratory tests of samples from the Lyons Mine were conducted at temperatures of 22.5°, 60°, 100°, and 200° C for axial loads of 2000, 4000, 6000, 8000, and 10 000 psi at each temperature. From these tests, it was observed that the deformation of the pillars increases markedly with increasing loads. However, even more significant is the greatly accelerated creep rates of the salt at elevated temperatures. An empirical relationship between creep, stress, temperature, and time has been developed from the tests. Model tests, verified by measurements in salt mines, show that thin shale beds, which commonly occur with bedded salt deposits, cause greatly accelerated rates of deformation in excavated cavities when they occur in the pillars at the roof and floor interfaces. In comparing the deformational behavior of salt from mines at Lyons and Hutchinson, Kansas; Retsof, New York; Detroit, Michigan; Grand Saline, Texas; Cote Blanche, Louisiana; and Asse, Germany, it was found that the general deformational behavior is the same; however, some variations in the rates of deformation were observed. Creep rates were also found to vary with the width-to-height ratios of pillars as well as with pillar shapes.

References

[1] Committee on Waste Disposal, Division of Earth Sciences, Disposal of Radioactive Wastes on Land. National Academy of Sciences-National Research Council Publication 519, Washington, D. C. (1957).

[2] Bradshaw, R. L. et al.: Ultimate Storage of High-level Waste Solids and Liquids in Salt Formations, in Treatment and Storage of High-level Radioactive Wastes, 153–175, International Atomic Energy Agency, Vienna (1963).

[3] Bradshaw, R. L. et al.: A Concept and Field-scale Test of Disposal of High Activity Power Reactor Wastes in Salt Mines, Transactions of the American Nuclear Society 7 (2), 399–400 (1964).

[4] Parker, F. L., L. Hemphill, and J. Crowell: Status Report on Waste Disposal in Natural Salt Formations, ORNL-2560, Oak Ridge National Laboratory, Oak Ridge, Tennessee (1959).

[5] Medwenitsch, W.: Geological Institute, University of Vienna, Vienna, Austria, personal communication with R. L. Bradshaw (Oak Ridge National Laboratory) (1962).

[6] Dellwig, L. F.: Flowage in Rock Salt at Lyons, Kansas. Kansas State Geological Survey Bulletin *130,* Part 4, 165–175 (1958).

[7] Bradshaw, R. L., J. J. Perona, and J. O. Blomeke: Demonstration Disposal of High-level Radioactive Solids in Lyons, Kansas, Salt Mine: Background and Preliminary Design of Experimental Aspects, ORNL-TM-734, Oak Ridge National Laboratory, Oak Ridge, Tennessee (1964).

[8] Bradshaw, R. L., et al.: Disposal of High Activity Power Reactor Wastes in Salt Mines: A Concept and Field Scale Demonstration, Nuclear Structural Engineering 2 (4), 438–446 (Oct. 1965).

[9] Boegly, W. J., Jr., et al.: Disposal of High Activity Power Reactor Wastes in Salt Mines: Mine Renovations Required for Project Salt Vault, Nuclear Engineering and Design (in press).

[10] Schaffer, W. F., Jr., et al.: Project Salt Vault: Design of Equipment. Nuclear Engineering and Design (in press).

[11] Lee, W.: Stratigraphy and Structural Development of the Salina Basin Area. Kansas State Geological Survey Bulletin *121,* 167 (1956).

[12] Pierce, W. G. and E. I. Rich: Summary of Rock Salt Deposits in the United States as Possible Storage Sites for Radioactive Waste Materials. United States Geological Survey Bulletin *1148,* 38–41 (1962).

[13] Serata, S.: Continuum Theory and Model of Rock Salt Structures, Second Symposium on Salt (Jon L. Rau, editor). The Northern Ohio Geological Society, Inc., Cleveland, Ohio, 1–17 (1966).

[14] Obert, L. E.: Deformational Behavior of Model Pillars Made from Salt, Trona, and Potash Ore, in Proceedings of the Sixth Symposium on Rock Mechanics, Rolla, Missouri, 539–560 (1964).

[15] Bradshaw, R. L., W. J. Boegly, Jr., F. M. Empson: Correlation of Convergence Measurements in Salt Mines with Laboratory Creep Test Data, in: Proceedings of the Sixth Symposium on Rock Mechanics, Rolla, Missouri, 501–514 (1964).

[16] Bradshaw, R. L. et al.: Disposal in Natural Salt Formations, in Health Physics Division Annual Progress Report for Period Ending July 31, 1967, ORNL-4168, Oak Ridge National Laboratory, Oak Ridge, Tennessee, 18–31 (1967).

Address of the authors: T. F. Lomenick and R. L. Bradshaw, Health Physics Division, Oak Ridge National Laboratory, P.O.B. X, Oak Ridge, Tennessee 37831, U.S.A.